Analysis of the global maritime transportation system as a layered network

David L. Alderson, Daniel Funk & Ralucca Gera

Journal of Transportation Security

ISSN 1938-7741

J Transp Secur
DOI 10.1007/s12198-019-00204-z

Journal of Transportation Security
https://doi.org/10.1007/s12198-019-00204-z

Analysis of the global maritime transportation system as a layered network

David L. Alderson [1] · Daniel Funk [2] · Ralucca Gera [3]

Received: 7 November 2018 / Accepted: 8 September 2019/Published online: 28 November 2019

Abstract
We model the global maritime transportation system as a multilayer network of sea routes and land routes that work together to deliver cargo on a global scale. The nodes of this network represent seaports and maritime chokepoints, and the arcs represent route segments at sea or on land, respectively. We construct our network using free, publicly available data from online sources, and we reverse engineer the global demand for container cargo transport. We use this layered network to identify important nodes from a connectivity standpoint. We also develop a flow-based model that directs the aggregate movement of goods between ports on the shortest and/or cheapest available route, and uses re-routing strategies if a route segment becomes impassable for container ships. We use this model to assess the impact of the loss of one or more container ports or maritime chokepoints. Using the base case of no disruptions, we measure the amount of goods that have to be re-routed in case of each disruption and the corresponding "cost" of doing so. Collectively, these results present a novel view of the security of transportation supply and set the stage for future work examining the global resilience of maritime transport systems.

Keywords Maritime network · Critical node · Centrality · Network flow · Interdiction · Resilience

✉ David L. Alderson
dlalders@nps.edu

Daniel Funk
danielfunk@outlook.de

Ralucca Gera
rgera@nps.edu

[1] Naval Postgraduate School, Monterey, CA, USA

[2] German Army, Oldenburg, Germany

[3] Naval Postgraduate School, Monterey, CA, USA

Introduction

The global economy is heavily dependent on the efficient and reliable transportation of cargo containers. The movement of these containers is facilitated by a *global maritime transportation network (GMTN)* that consists of seaports, waterways, and landside connections. This system has evolved over the last several decades to minimize transportation costs and is now highly optimized for efficiency. As long as there are no disruptions to the global system, all cargo sent through the system arrives at its destination without delay. But unforeseen events, like container port closures (either deliberate or non-deliberate) or disruptions at maritime chokepoints, can force the shipping companies to choose different routes for the cargo, resulting in higher costs or perhaps even making it even impossible for some cargo to be delivered. Understanding the way in which the GMTN adapts or fails in the presence of such disruptions is important for assessing and improving the *security of supply* for a variety of industries and other operations that fundamentally depend on it.

The evolution of the current system is commonly attributed to two main driving forces. First, lower labor and manufacturing costs in certain parts of the world have led to outsourcing of production and a dramatic increase in international commodity trade. According to the World Trade Organization (2007), the growth in world trade increased from 1950 to 2005 by a factor of 27. As a result, there has been a growing need for transportation of more and more goods across the world at cheaper costs. Second, the development of the standard shipping container by the International Standards Organization (ISO) in the late 1950s revolutionized global shipping. The standardization of maritime transport, through the use of containers and increased mechanization of the container handling in seaports, reduced the needed manpower by about 90% and the container handling cost by about 80% (Huber 2014). The GMTN took advantage of that development and grew very quickly. Within this global network, some seaports had logistics advantages—for example, convenient geographical location and/or better developed landside transport connections—and therefore, they were favored by the transportation companies and became regional hub ports. In a manner consistent with the "rich get richer" principle, these few ports grew faster than the others, became global "megaports" and are today essential for the worldwide logistics.

Today, nearly a half of the worldwide container handling is transshipped through the top twenty global megaports (Bruns et al. 2013). Therefore, today's megaports are not only important for the surrounding regions, but also for the entire GMTN due to potential vulnerabilities that they might create. It is widely believed that the loss of one or more megaports—as could happen from a natural disaster, terrorist attack, infrastructure failure, or mere capacity limitations—could have severe global consequences. One famous example is the West Coast port labor slowdown and lockout in 2002, when negotiations of labor agreements caused a stop of port operations for ten days. As Los Angeles Times reports: "It took the West Coast ports 100 days to return to normal operations" (Khouri 2015). It is believed a longer port shutdown would have caused a shutdown of production lines in the U.S. and emptied the shelves in the malls (Cohen 2002). More recently, Hanjin Shipping, the then-seventh-largest deep sea cargo transportation carrier in the world, filed for bankruptcy in August 2016, leaving 80 cargo ships, their respective crews, and roughly $14 billion worth of cargo stranded at sea or outside seaports for days or weeks (Cruz 2016).

The importance of the GMTN is now well recognized, but much like other critical infrastructure systems, such as electric power, water, or telecommunications, its continued operation is largely taken for granted. Flynn et al. (2017) highlight this point and study the vulnerability of the global supply system, cautioning that it has the potential to be targeted or exploited by terrorist organizations in the way that other systems, such as passenger aviation, air cargo, and mass transit, have been. However, to date there have been relatively few studies that address the operational resilience of this system.

This paper takes a first step in this direction by modeling a GMTN as a multilayer network of sea routes and land routes that work together to deliver cargo on a global scale. The nodes of this network represent seaports and maritime chokepoints, and the arcs represent route segments at sea or on land, respectively. The two layers are given by the sea routes versus the land routes, while all the nodes are present in both layers. We construct our network using free, publicly available data from online sources, and we reverse engineer the global demand for container cargo transport. We use this layered network to identify important nodes from a connectivity standpoint. We also develop a flow-based model that directs the aggregate movement of goods between ports on the shortest and/or cheapest available route, and uses re-routing strategies if a route segment becomes too congested or impassable for container ships. We use this model to assess the impact of the loss of one or more container ports or maritime chokepoints. Using the base case of no disruptions, we measure the amount of goods that have to be re-routed in case of each disruption and the corresponding "cost" of doing so. Collectively, these results present a novel view of potential disruptions and their impact on the security of transportation supply on a global scale. It also sets the stage for future work examining the global resilience of maritime transport systems.

Past work

Transportation networks are a common topic of study for analyzing network structure, performance, resilience and other measures of interest. Transportation systems (air, land and at sea) have received considerable attention in the academic literature. For example, the Transportation Research Board (TRB) is a unit of the U.S. National Academy of Sciences, Engineering and Medicine that coordinates and manages transportation research, conducts policy studies, and publishes reports on a variety of issues facing the transportation industry. See Nagurney (2006) and Rodrigue et al. (2017) for an overview of issues involving economics and geography of transportation systems. In this section, we highlight selected work from this vast literature that is most relevant to the current study.

Ports and port operations Because ports play a critical role in the movement of containerized cargo, significant efforts have been directed at their modeling and analysis. Pidgeon (2008) models the seven major ports of the U.S. West Coast to evaluate potential disruptions and the corresponding costs inflicted on the shipping industry. He examines the bottlenecks within each port's infrastructure that can be vulnerable to a transportation security incident (TSI), including earthquake, terror attack, and worker lockout. Using these predefined scenarios, he estimates the impact on vessel queue time and incremental costs, as well as downstream impacts on the U.S.

economy as a whole. He considers the potential to re-route ships to different destination ports, and provides recommendations for future investments to alleviate port congestion.

Bencomo (2009) extends this work to consider infrastructure throughout the U.S. and includes data for container flows between 46 countries and the U.S. ports. Using an Attacker-Defender model, introduced by Brown et al. (2006), he identifies the worst-case interdictions to the network, even after cargo has been rerouted. Martagan et al. (2009) use a simulation-based approach to model the potential impact of port disruptions on the GMTN. Focusing on seven ports within the U.S., they develop a queueing type of model that simulates the process by which ships enter a port, unload cargo, load cargo, and depart the port. In a manner similar to Pidgeon (2008), when a port is disrupted, ships can be re-routed to alternate ports. The authors study the potential benefit of this re-routing strategy, which we consider in this current research as well.

Several studies have also focused in more detail on the operations within a port. Specifically, De la Cruz (2011) models operations in the Port of Honolulu and the broader Hawaii Maritime Transport System at the level of individual terminals and cranes, developing an optimization-based model to assess the throughput capacity of this system under normal circumstances and during adverse events. He considers alternate strategies to mitigate capacity shortfalls and system vulnerability, as well as to improve the overall operational resilience of the system. Similar techniques have been applied to the Port of Pittsburgh (Onuska 2012), the Port of Los Angeles (Mintzer 2014), and the Port of Anchorage (Wenke 2015).

Global sea route networks The study of maritime container transportation at the regional or global scale has focused also on the network features of the system.

The growing field of *network science* has developed a variety of tools and techniques for understanding the structure and behavior of systems based on their connectivity; see Newman (2010) for a comprehensive introduction. Focusing on the connectivity of seaports, as defined by the cargo ships that travel between them, Wang and Cullinane (2016) develop a measure of "port centrality" (based on other well-established measures of degree centrality, closeness centrality, and between-ness centrality, discussed below) that captures the accessibility to other ports. Particularly for the GTMN, Wang and Wang (2011) argue that, from topological point of view, the GTMN has transitioned from a "multi-port calling system" to 44 regional hub-and-spoke subsystems with a hierarchical structure, demonstrating a great diversity in linkage coverage (probability that one port is connected with any other port) among different regions. They report that based on centrality values, the GTMN network is dominated by the ports of Antwerp, Singapore, and Hong Kong that act as regional hubs.

The sea route network has also been analyzed using network flow models with the intent to characterize the global effect that ports play in the network's resilience. Partial reviews of the literature on disaster resilience of transportation infrastructure and ports are available from Madhusudan and Ganapathy (2011) as well as Faturechi and Miller-Hooks (2014). Chen and Miller-Hooks (2012) study the resilience of an intermodal freight transport network, considering specifically activities that can be taken following a disaster to mitigate performance. They assess resilience using a two-stage, stochastic mixed-integer program for several canonical synthetic networks (i.e., a complete graph, a random graph, and a grid network). Miller-Hooks et al. (2012) extend this work to the study the U.S. rail-based intermodal container transportation network, by analyzing resilience, preparedness and recovery. They solve for the best portion of a fixed budget to spend on preparedness and the portion to save for the recovery actions after the disaster.

Kaluza et al. (2010) take a global view by modeling GTMN as a multilayer network, aggregating the transportation flows of goods by type as well as by their specific physical characteristics, each type being represented by a layer. They analyze this multilayer network for ship movements, obtained from their automatic identification system (AIS) transmissions, to understand patterns of global trade and bioinvasion; these were further studied by Ruiz et al. (2000) and Drake and Lodge (2007).

The resilience of GMTN has been studied by looking at changes in the properties and structure of the network following a disruptive event (e.g., port attack). Ducruet and Notteboom (2012) show that the global shipping network is robust, in the sense that the centrality of key nodes changes very little even when global trade shifts following changes in network structure. Garcia Olalla (2012) models the GMTN using a flow network that includes artificial transition points (group nodes) that bundle all flow to and from multiple seaports within a region; aggregate movement between these transition points then follows a type of "maritime highway." He analyzes resilience by considering one or more disruptions along route segments, expressed either as penalties in time or cost, for ships that must avoid the interdicted routes. Jiang et al. (2015) also use travel time and port capacity models to study the global influence of a port based on its connectivity.

Other global transport networks The air transportation network has been studied by several researchers who have identified its scale-free structure, community structure, and central nodes (Guimerá et al. 2005). In particular, the European Airline Transportation Network has received considerable attention: the anomalous centrality distribution was studied by Guimerá et al. (2005); the most connected cities versus central cities was investigated by Guimerá and Amaral (2004); the multilayer structure and emergence of a single layer was considered by Cardillo et al. (2013); a synthetic multilayer network was created by Basu et al. (2015); and network flows in multilayer networks was studied by De Domenico et al. (2015).

Network model construction

We begin our analysis with the construction of a network model for global maritime shipping. To the best of our knowledge, there does not exist a single standard representation for the global maritime transportation network nor is there is a single non-proprietary repository from which one can obtain complete data to support its creation. Therefore, an essential part of our work is the collection and aggregation of data from various sources. In order to collect a large amount of information housed at a variety of different online resources, we employ "web scraping" (also known as "screen scraping" or "web harvesting") to automatically gather data from the Internet; see Mitchell (2015) for general background and Funk (2017) for details of the technique used here.

This section details the assumptions and methodology used to create a network abstraction of the global maritime transportation network. In our analysis, we concentrate solely on the transportation of containers. Although there are potentially valuable insights from an analysis of transportation for other goods (e.g., oil and bulk material), these are not covered here.

Network nodes: Ports and maritime chokepoints

We introduce a global model that captures the maritime system such that we can analyze its resilience based on one or several local attacks. We thus view the maritime transport system as a network of ports that facilitate the movement of containerized goods on a global scale. We consider two distinct types of nodes.

Our first type of node is a seaport, which we define as a location with the ability to move container cargo between container ships and land. The global maritime transportation network contains hundreds of container seaports worldwide, but many of these are small and do not handle much cargo. We focus on the most important container ports of the world, measured in terms of the amount of cargo throughput. In all cases, we use twenty-foot equivalent units (TEUs) as the unit of measure.

The Central Intelligence Agency (CIA) produces an annual World Factbook, which contains various statistics about the countries of the world, published as a permanently available online resource (Central Intelligence Agency 2017), including information about ports and terminals. Specifically, we use an automated program to scrape systematically the online version for every container seaport and its annual throughput for every country. The currently available throughput data is mostly for the year 2011, with few exceptions of 2010 and 2012. There are a total of 94 container seaports from 58 different countries, listed in Table 1.

The second type of node is a maritime chokepoint, representing areas with restricted throughput and/or high concentration of ships, such as straits and canals. Because sea traffic is naturally constrained in these places, chokepoints create potential vulnerabilities to the movement of containers across the entire network.

There are many places throughout the world that could potentially be considered maritime chokepoints. Komiss and Huntzinger (2011) choose maritime chokepoints based on established oil tanker transportation routes. These are located primarily on the main routes from the Middle East and include the Strait of Hormuz, the Strait of Malacca, the Suez Canal, Bab el-Magdeb, the Turkish Straits (Dardanelles), and the Panama Canal. Noer and Gregory (1996) consider chokepoints of the trade routes and strategic straits in the Australasian Mediterranean Sea, which includes the Lombok Strait and the Sunda Strait. Other considerations for chokepoints take into account less frequented but still important chokepoints like the Magellan Passage or the Dover Strait.

Based on these considerations, along with our previous selection of the container ports, we choose the following 26 maritime chokepoints (Table 2), which cover the routes between our selected ports.

In total, we have 120 container seaports and maritime chokepoints. Each seaport represents a source and/or destination for container cargo transport. Each chokepoint is a transshipment node through which cargo flows.

Table 1 Select container ports for our model, along with their annual throughout, measured in Twenty-Foot Equivalent Units (TEUs). Source: Central Intelligence Agency (2017)

Country	Port	Throughput
Argentina	Buenos Aires	1,851,701
Australia	Brisbane	1,004,983
Australia	Melbourne	2,467,967
Australia	Sydney	2,028,074
Bahamas	Freeport	1,116,272
Bangladesh	Chittagong	1,392,104
Belgium	Antwerp	8,664,243
Belgium	Zeebrugge	2,207,257
Brazil	Itajai	983,985
Brazil	Santos	2,985,922
Canada	Metro Vancouver	2,507,032
Canada	Montreal	1,362,975
China	Dalian	6,400,300
China	Ningbo	14,719,200
China	Qingdao	13,020,100
China	Port of Shanghai	31,739,000
China	Tianjin	11,587,600
China	Guangzhou	14,260,400
China	Shenzhen	22,570,800
Colombia	Cartagena	1,853,342
Ecuador	Guayaquil	1,405,762
Egypt	Alexandria	1,108,826
Egypt	Port Said	3,755,796
Franco	Le Havre	2,215,262
Germany	Bremerhaven	5,915,487
Germany	Hamburg	9,014,165
India	Chennai	1,558,343
India	Jawaharlal Nehru Port	4,307,622
Indonesia	Tanjung Priok	5,617,562
Iran	Bandar Abbas	2,752,460
Ireland	Dublin	1,931,001
Israel	Ashdod	1,176,000
Israel	Haifa	1,238,000
Italy	Genoa	1,847,648
Italy	Gioia Tauro	2,264,798
Italy	La Spezia	1,307,274
Jamaica	Kingston	1,724,928
Japan	Kobe	2,725,304
Japan	Nagoya	2,471,821
Japan	Osaka	2,172,797
Japan	Tokyo	4,416,119

Table 1 (continued)

Country	Port	Throughput
Japan	Yokohama	2,992,517
Korea, South	Busan	16,163,842
Korea, South	Kwangyang	2,061,958
Korea, South	Incheon	1,924,644
Lebanon	Beirut	1,034,249
Malaysia	Penang	1,202,180
Malaysia	Port Klang	9,435,403
Malaysia	Tanjung Pelepas	7,302,461
Malta	Marsaxlokk	2,360,000
Mexico	Manzanillo	1,992,176
Mexico	Lazaro Cardenas	1,242,777
Morocco	Tangier	2,093,408
Netherlands	Rotterdam	11,876,920
Oman	Salalah	3,200,000
Pakistan	Karachi	1,545,434
Panama	Balboa	3,232,265
Panama	Colon	2,390,976
Panama	Manzanillo Int. Terminal	2,391,066
Peru	Callao	1,616,365
Philippines	Manila	3,342,200
Puerto Rico	San Juan	1,484,595
Russia	Saint Petersburg	2,365,174
Saudi Arabia	Jeddah	4,010,448
Saudi Arabia	King Abdul Aziz Port	1,492,315
Singapore	Singapore	31,649,400
South Africa	Durban	2,712,975
Spain	Las Palmas	1,287,389
Spain	Algeciras	3,608,301
Spain	Barcelona	2,033,747
Spain	Valencia	4,327,371
Sri Lanka	Colombo	3,651,963
Taiwan	Keelung	1,749,388
Taiwan	Kaohsiung	9,363,289
Taiwan	Taichung	1,383,578
Thailand	Bangkok	1,305,229
Thailand	Laem Chabang	5,731,063
Turkey	Mersin	1,126,866
Turkey	Ambarli	2,121,549
United Arab Emirates	Dubai	12,617,595
United Arab Emirates	Khor Fakkan	3,234,101
United Kingdom	Southampton	1,324,581
United Kingdom	Felixstowe	3,248,592

Table 1 (continued)

Country	Port	Throughput
United Kingdom	London	1,932,000
United States	Long Beach	6,061,091
United States	Los Angeles	7,940,511
United States	Oakland	2,342,504
United States	Seattle	2,033,535
United States	Houston	1,866,450
United States	New York	5,503,485
United States	Savannah	2,944,678
United States	Hampton Roads	1,918,029
Vietnam	Hai Phong	1,018,794
Vietnam	Saigon Port	3,071,777

Network edges: Sea and land

Whereas nodes in our network represent physical locations on the globe, we use network edges in our model to represent the abstract movement between nodes rather than any specific physical route.

Although our primary interest is in studying the movement of cargo by sea, we also consider potential movement of cargo by land, as an alternative in situations where sea transport might be restricted. Thus, ours is a multiplex network model that has two "layers", one representing sea transport (i.e., the sea layer) and another representing land transport (i.e., the road layer). Figure 1 depicts portions of the sea and road layers as visualized in Google Earth.

We now describe the construction of network edges for these two layers.

Sea layer

The edges of the sea layer represent the maritime ship routes between container ports and/or chokepoints. The natural spatial pattern of the seaport locations around the world defines the structure of the sea layer. The seaports are always situated at one specific body of water (e.g., the Atlantic Ocean or the South China Sea). By construction, the maritime

Table 2 Maritime chokepoints included in our representation of the maritime transportation network

Bering Strait	Suez Canal	Taiwan Strait	Great Britain
Davis Strait	Strait of Gibraltar	Luzon Strait	(northern tip)
Barents Sea	Cape of Good Hope	Magellan Passage	Trinidad and Tobago
Strait of Hormuz	Sunda Strait	Dardanelles	(northern tip)
Strait of Malacca	Lombok Strait	Dover Strait	Yucatan Channel
Bab-el-Mandeb	Tones Strait	Øresund	Windward Passage
Panama Canal	Makassar Strait	Great Australian Bight	Mona Passage

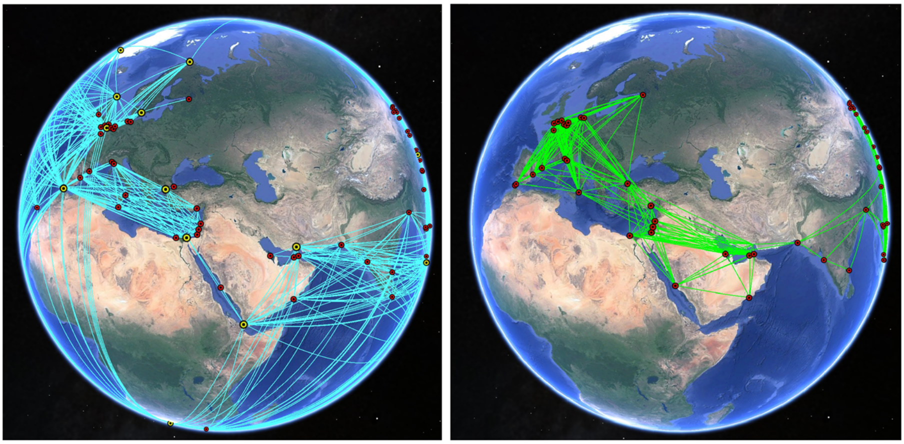

Fig. 1 Portions of the sea layer (left) and road layer (right) as visualized in Google Earth. The red points are the container ports and the yellow points represent the maritime chokepoints. The lines represent the direct connections in between, visualized here simply as straight lines

chokepoints always separate the single bodies of water from their neighbors. As a result, the container ports are subdivided into eleven groups, corresponding to the adjacent bodies of water: Pacific Ocean, Atlantic Ocean, Indian Ocean, Caribbean Sea, North Sea, Baltic Sea, Mediterranean Sea, Sea of Marmara, Red Sea, Persian Gulf, and South China Sea.

Because the maritime chokepoints in the network act as transshipment nodes for longer routes, we only need to model the connections between seaports of each body of water separately. Within each body of water, all possible pairwise connections are implemented in the model, which makes each subnetwork of each body of water a clique (i.e., a fully connected subset of nodes). The chokepoint nodes always count as members of both neighboring cliques.

Figure 2 illustrates the adjacency matrix of the sea layer. Each block in the matrix represents a different body of water and can be easily recognized in the white and grey areas. The blue area shows the connections to, from and between the chokepoints. There are a total of 1518 edges in the sea layer.

Road layer

The road layer plays a subordinate role in our network model; it is implemented to provide a possibility of alternate routes for goods transported by sea. Whenever there is a situation where the destination container port is out of order or a maritime chokepoint along the route is impassable, a transfer to landside transportation of the road can be considered.

For this layer, the nodes correspond to seaports, omitting the maritime chokepoints as they have a meaning only for sea routes. Although it is theoretically possible to travel by car between France, South Korea and South Africa without using any ferries, not every road connection between two ports is required. Since road transportation is expensive, it would only be used to bypass relative short distances, compared to those within the sea layer. The purpose of the road layer will be either to deliver goods to the

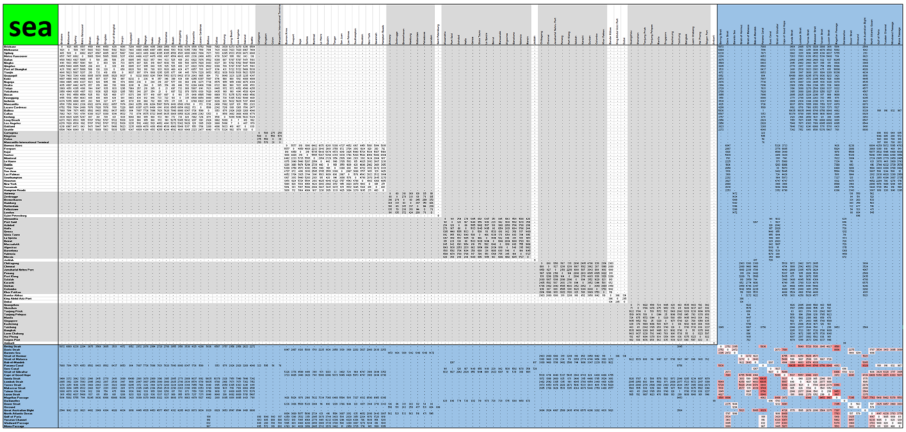

Fig. 2 Adjacency matrix of the sea layer. The block structure (in white and grey areas) results from the fully connected nature of ports on the same body of water. The blue area shows interconnection of chokepoints between each body of water

final destination or to the next functional seaport to switch back to ship transportation. Therefore, we impose a maximum threshold for the road connections at 2000 nautical miles, ignoring larger distances in the adjacency matrix.

Figure 3 provides a global overview of the layer. Here, North and South America are recognizable on the left side with four connected components. Furthermore, there is a large component connecting Europe, Northern Africa and Asia. Three other components are in Taiwan, Japan and Australia, resulting in a total of eight connected components. The resulting road layer contains 365 edges that connect the 83 seaports.

Edge distances

To make the model realistic, we seek for each edge a weight attribute that represents the cost of using the edge on a route. In general, the relative costs for different modes of transport are dramatically different. For example, according to Rodrigue et al. (2017) the average transport cost per ton-mile (in 1995 dollars) for different modes were as follows: water ($0.01), rail ($0.03), truck ($0.25), and air ($0.59). Zeihan (2014, p.12)

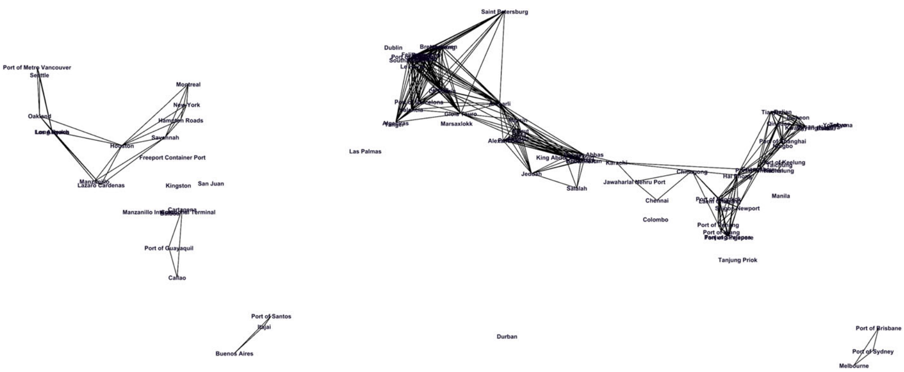

Fig. 3 Graphical representation of the road layer, arranged approximately on a Cartesian map of the world

similarly reports, "Modern container ships can transport goods for about net 17 cents per container-mile, compared to semitrailer trucks that do it for net $2.40, including the cost of the locomotion mode as well as operating costs in both instances." We adopt these values as relative costs for each layer. In general, the biggest component of transport cost is the amount of energy required, which depends on economies of scale for each mode as well as the distance travelled.

To obtain the distance between pairs of nodes within each of the sea and road layers, we collect real data using web scraping of public websites, in a manner similar to that described in Section 3; for details see Funk (2017). For the sea layer, we use the SeaRates website (SeaRates LP 2017). A potentially more accurate method for calculating shortest sea route distances would be to use the technique of Brown and Washburn (2017), but this was not considered here. For the road layer, we collect the road distances automatically from the websites for Bing Maps (Microsoft Corporation 2017) and Google Maps (Google 2017). We record all of our calculated distances in nautical miles for consistency.

We use an adjacency matrix for each layer to store its distance data. It has zeros on the main diagonal and is symmetric because we assume that the direction of a route between two nodes doesn't influence the actual travel distance.

We weight the edges in our multiplex network by the product of this real world travel distance and the relative cost factor for each mode of transport. Thus, our representation of the GMTN allows us to consider the relative cost of moving cargo in the sea layer and/or the road layer. In our subsequent analysis, we do not consider transportation by rail or air.

Centrality analysis

As noted above, one of the topics studied in transportation networks is the centrality of nodes. Centrality is a quantification of the intuitive notion of importance of a node in a network, the answer of what is central depends on what is of interest. The standard centrality measures can be classified as local versus global measures. The commonly used local centrality measures are (1) degree centrality, which measures importance within the 1-hop neighborhood, introduced by Shaw (1954); and (2) *H-Index*, used to evaluate the scientific output of a researcher, introduced by Hirsch (2005). The commonly used global centrality measures are (1) *closeness centrality*, which measures how close a node is to every other node, introduced by Sabidussi (1966); (2) *betweenness centrality*, which measures the percent of shortest paths for which each node acts as an intermediate node, introduced by Freeman (1977); and (3) different variations of decaying extensions of degree centrality based on the distance to the node in questions: *eigenvector centrality*, introduced by Stephenson and Zelen (1989); *Katz centrality*, introduced by Katz (1953); and *PageRank*, introduced by Brin and Page (2012).

In studying the centrality of nodes in the GMTN, we consider each layer in isolation, as well as the combination of the two layers. For each of the cases, we start by looking at connectivity before performing a deeper analysis. We begin by considering each network layer in isolation.

Basic connectivity properties

The sea layer as a whole is a collection of eleven cliques, each interconnected to others by one or more chokepoints. The biggest clique has 37 nodes representing the group of very connected ports in the Pacific Ocean. This layer also has a highly assortative community structure in terms of its node degree, with high-degree nodes connecting to other high-degree nodes, and low-degree nodes connecting to other low-degree nodes. The maximum degree centrality is 62, attained by several nodes representing maritime chokepoints connecting Pacific Ocean, the Indian Ocean, and the South China Sea, each of which contains many ports. The average degree of the sea layer is 25.3. Overall, this layer is a clustered graph, with a clustering coefficient value of 0.9 (out of a possible maximum of 1.0), which is very high. It thus presents a small world structure, with average shortest path length is 2.2 (meaning that, on average, ships have to pass 1.2 chokepoints travelling between two ports), and the longest shortest path within the layer has a length of five.

The road layer has very different connectivity properties, yet is still a small world. The average degree of this layer is approximately 8.8. The maximum degree centrality is 24 attained by Ambarli, Turkey; this node has a central location within its component, being connected to all European ports and some of the Asian ports, and it has the smallest degree of all nodes in the sea layer. The average shortest path length is 3, measured within each component. The overall clustering coefficient of the road layer is 0.87, which is still high. This is because of the five small components, each of which has a value of 1. The clustering coefficients for North America and Eurasia are 0.82 and 0.83, respectively. The high values follow from the fact of the selected threshold to introduce distance-based edges to our model. Because of that, nodes are mostly connected to others with a similar degree, like it is in the case in Europe, and there is no connection to the weakly connected Middle East.

Identifying central nodes

As a first attempt to identify which nodes are "important" in our network, we consider the degree centrality, closeness centrality and betweenness centrality. The distributions for the centralities of both layers appear in Fig. 4.

The degree centrality measures the number of one-hop connections, showing the importance of a node locally. For the sea layer, nodes with the highest degree centrality have a value of about 0.53; these correspond to the transition nodes between the Pacific Ocean, the Indian Ocean and the South China Sea, that have the highest node degree. Respectively, the nodes with the lowest degree have the lowest degree centrality of about 0.01. A similar situation can be observed within the road layer, where Ambarli has the highest centrality at about 0.29 and the nodes of the small connected components have the lowest value of about 0.02.

Closeness centrality of a vertex can be viewed as the efficiency of the vertex in spreading information to all other vertices. Thereby, the number of neighbors of a node is less important for the closeness centrality, but rather the number of nodes within a short distance from that node. The higher the closeness centrality is, the closer the node is to all others. For both the sea and road layer, the five nodes with the highest closeness centrality and highest degree centrality are the same (corresponding to the transition

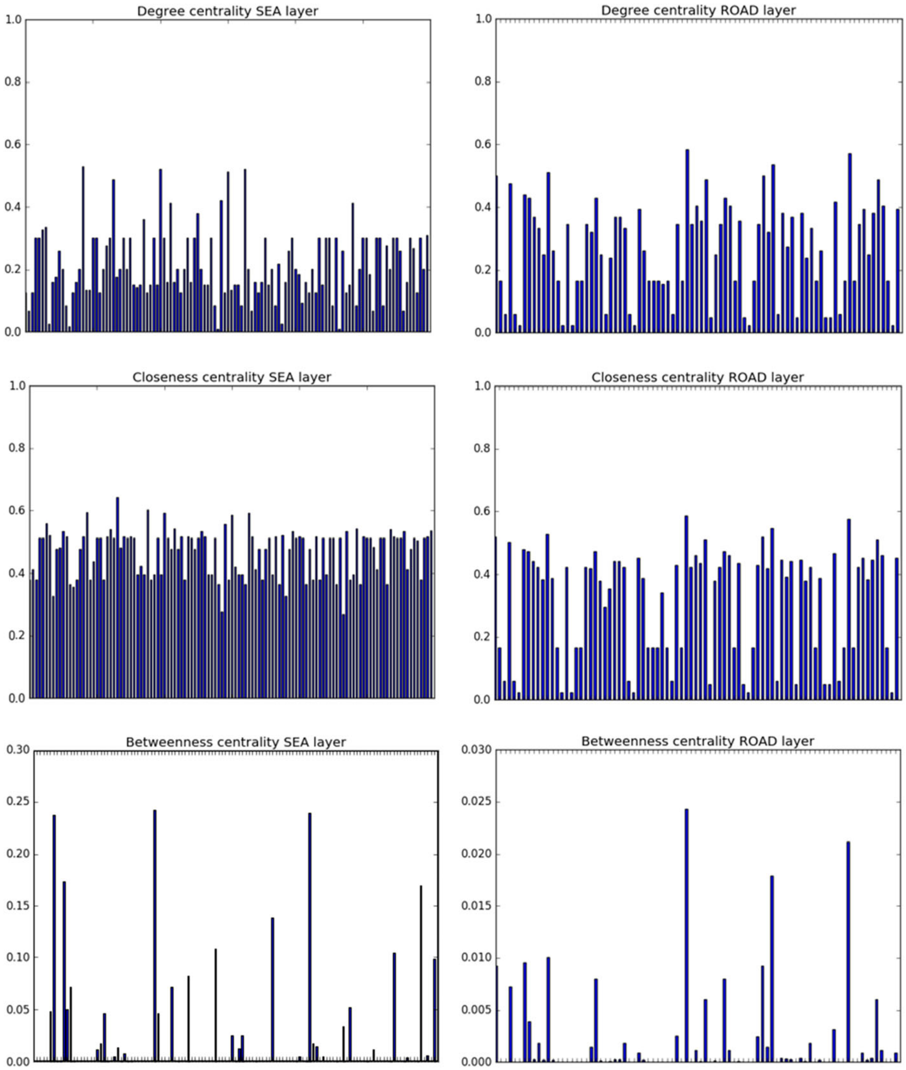

Fig. 4 Plots of centralities' distributions of the sea and the road layer, respectively. The vertical axes represent the centrality values on a scale from zero to one. The horizontal axes represent the network nodes in an arbitrary order, which is consistent across all plots

nodes between the Pacific Ocean, the Indian Ocean and the South China Sea), while the other nodes present different degree versus closeness ranking.

The betweenness centrality is useful when studying the flow through a network, for example, a flow of data packages or goods. To calculate the betweenness centralities in our network, we use the weights of the edges representing the real sea distances between the nodes. Within the sea layer, the Strait of Gibraltar, the Suez Canal and Bab-el-Mandeb are by far the most central nodes, as they are chokepoints on the shortest route between Asia and Europe. They are followed by the Strait of Malacca. Surprisingly, the Panama Canal has a smaller rank than maybe expected (its importance is based on its throughput, which is not taken into account in this centrality). For the road layer, Karachi, Shenzhen and Ambarli have the highest values, not surprisingly, since they act as hubs on many road routes in Asia and between Asia and Europe. In both layers, many nodes have a value of zero, which means that their geographical location does not qualify them as stops on routes between other nodes.

Network flow representation

A connectivity-based view of system structure can provide valuable insight, but the GMTN is more than a simple network. In particular, it is a system that has evolved over many years to deliver cargo reliably and at minimum cost. Its operations must satisfy the need to move goods from areas of supply to areas of demand, while traversing long distances and contending with capacity constraints at ports. Incorporating this operating context into the study of a network-based infrastructure can be fundamental to understanding its essential features, particularly when it comes to identifying vulnerabilities and proposed investments (see Alderson 2008, Alderson and Doyle 2010, for detailed discussions).

In this section, we expand our network model to reflect the flow of cargo through the system. Specifically, we represent the GMTN as a multi-commodity, minimum-cost network flow problem, in which the directed arcs in each layer of the network have a per-unit flow cost as well as a capacity. For an introduction to the basic mathematical framework for representing network models, see Ahuja et al. (1993). We additionally apply the modeling techniques in Alderson et al. (2015) to evaluate system behavior and operational resilience, both under normal conditions and during exigencies. We detail the assumptions, formulation, and solution below.

Modeling port and chokepoint capacity

Container ports and canals in the real world can only process a finite number of ships and containers in a fixed time period. This number is referred to as their capacity. A study of the The Tioga Group (2010) provides a broad overview over port capacities of the major U.S. ports, subdivided in North Atlantic, South Atlantic and Gulf Coast regions. The container terminal capacity is measured in five "dimensions" such as berth length and depth, number of berths and cranes, container yard acreage and the operating hours of the ports (number of shifts). The study comes to a conclusion that based on the five "dimensions," ports have different capacities and the distribution of strengths and weaknesses over the "dimensions" is different in each port. But in general, each of the three regions on its own could handle roughly double of the actual throughput before reaching its capacity constraints. Based on this study, we assume that each port in our network has a capacity equal to double the normal throughput (measured in TEUs).

In order to model capacity at ports and chokepoints, we adjust our existing network as follows. First, we replace each undirected edge by two directed arcs, one in each direction. Second, we use "node splitting"—where we replace a node with two copies separated by a single directed arc—on ports and chokepoints. The example in Fig. 5 (left) illustrates the situation prior to node splitting, with undirected edges between the nodes. It shows two container ports that have a direct sea connection in between (the blue edge), a connection via a maritime chokepoint and a road connection (the green edge). Figure 5 (right) depicts the same situation after node splitting: each edge is replaced by two bidirectional arcs with the exception of chokepoints. These are now split in an incoming and an outgoing node with exactly one arc in between.

We can implement port capacity in the seaward or landward direction by restricting the capacity on the corresponding directed arc between the split nodes. Similarly, we can implement capacity through a chokepoint by restricting the flow on the directed arc. At the extreme, we can disable a port or chokepoint by blocking all flow along these directed arcs.

One way to implement a disruption on an arc could be remove it from the network, or perhaps reduce its capacity to zero (which would have the same effect). However, this has the potential to create infeasible network flows and can be problematic when solving iteratively for solutions. Instead, we use "cost-based interdiction" and increase the usage cost of each targeted arc as described in Alderson et al. (2014). In this way, a targeted arc becomes too expensive and will not be considered for a solution.

Modeling supply and demand

As previously noted, Table 1 lists the annual throughput in each of our ports. We augment this with additional data about the current export and import partners of the countries that are represented in the model. Specifically, Table 10 in the Appendix lists the total exports and imports by country, and Table 11 in the Appendix shows the export and import partners of each country. The countries without ports in our model

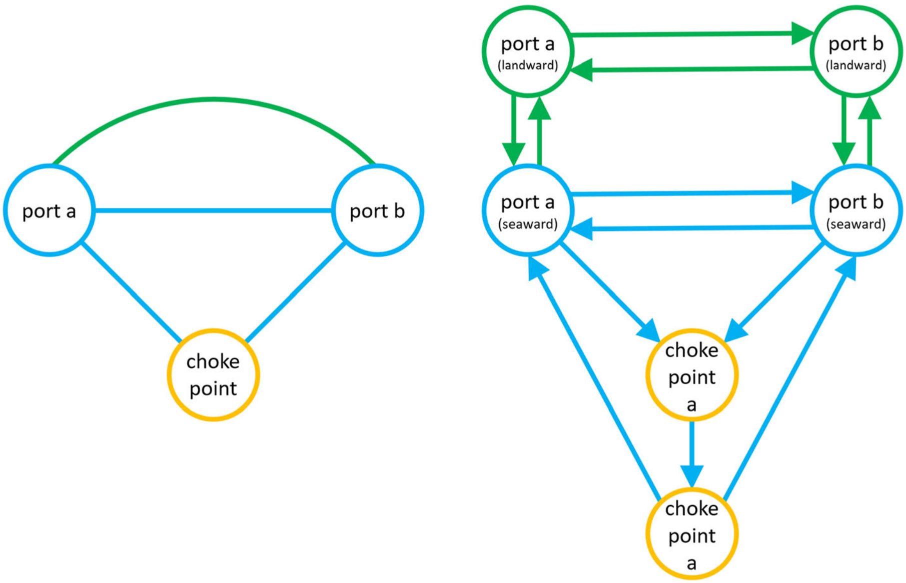

Fig. 5 Two representations of layered networks. Left: A layered network consisting of sea connections (blue edges) and road connections (green edges). Edges are undirected. Right: The same network with directed arcs and "node splitting" to separate each port into a seaside node and a landside node, and to separate each chokepoint into a inbound node and an outbound node. By placing flow constraints on the arcs connecting the split nodes, we can restrict the capacity of flows through these nodes

have been filtered out. Because there is no data provided for Puerto Rico, we assume the same partners there as for the United States. Using this data, we derive approximate cargo flows between different pairs of ports. We represent this data as a matrix of flows between points of supply and points of demand within the network.

In our model, we do not distinguish between different types of cargo (everything is simply measured in terms of TEUs), however we differentiate cargo with different destinations as different types of *commodities*. That is, we assume that cargo destined for Los Angeles cannot be substituted for cargo destined for Oakland. Thus, our matrix of cargo flows defines the overall demand for cargo movement by commodity for the GMTN.

Mathematical formulation

We next provide the mathematical formulation of the multi-commodity linear optimization model that minimizes the total cost of the global cargo flow. It preserves the balance of flow at the nodes, allows for shortfall (undelivered cargo) at individual nodes, and is instrumented to easily accommodate the interdiction (failure, closure) of individual arcs.

Indices and Sets

$n \in N$	nodes (alias i, j)
$s \in S \subset N$	sea nodes
$r \in R \subset N$	road nodes
	$N = S \cup R; S \cap R = \varnothing$
$(i, j) \in A$	directed arc from node i to node j

Data [Units]

c_{ij}	per unit cost of traversing arc $(i, j) \in A$ [dollars/TEU]
u_{ij}	upper bound on total directed flow on arc $(i, j) \in A$ [TEU]
$\hat{x}_{ij}$	1 if arc $(i, j) \in A$ interdicted, 0 otherwise [binary]
q_{ij}	per unit penalty cost of traversing interdicted arc $(i, j) \in A$ [dollars/TEU]
d_n^r	demand at node $n \in N$ for cargo originating from node $r \in R$ [TEU] (supply if $d_n^r < 0$)
p_n	per unit penalty cost for demand shortfall at node $n \in N$ [dollars/TEU]

Decision Variables [Units]

Y_{ij}^r	flow on arc $(i, j) \in A$ of cargo originating from node $r \in R$ [TEU]
Z_n^r	shortfall of cargo originating from node $r \in R$ at node $n \in N$ [TEU]
E_n^r	excess of cargo originating from node $r \in R$ at node $n \in N$ [TEU]

Formulation

$$\min_{Y,Z} \sum_{r \in R} \sum_{(i,j) \in A} \left[\left(c_{ij} + q_{ij} \hat{x}_{ij} \right) Y_{ij}^r \right] + \sum_{r \in R} \sum_{n \in N} \left[p_n \left(Z_n^r + E_n^r \right) \right] \tag{D0}$$

$$\text{s.t.} \quad \sum_{(i,n)\in A} Y_{in}^r - \sum_{(n,j)\in A} Y_{nj}^r + Z_n^r - E_n^r = d_n^r \qquad \forall n \in N, \forall r \in R \qquad \text{(D1)}$$

$$0 \le \sum_{r\in R} Y_{ij}^r \le u_{ij} \qquad \forall (i,j)\in A \qquad \text{(D2)}$$

$$Y_{ij}^r \ge 0 \quad \forall (i,j)\in A, \qquad \forall r\in R \qquad \text{(D3)}$$

$$Z_n^r \ge 0 \quad \forall n\in N, \qquad \forall r\in R \qquad \text{(D4)}$$

$$E_n^r \ge 0 \quad \forall n\in N, \qquad \forall r\in R \qquad \text{(D5)}$$

Discussion

The objective function (D0) is a summation of costs that are generated by the model: the combined flow cost over sea and road connections and the penalty cost for having a demand shortfall or excess at some nodes. The constraint (D1) ensures the balance of flow at each node and for each commodity, setting the incoming and the outgoing flow, the shortfall and the excess equal to the demand at that node. Constraints (D2), (D3), (D4) and (D5) define bounds on decision variables.

In practice, we only implement arc capacities u_{ij} on the arcs between "split" nodes (i.e., seaports and chokepoints).

This is a prescriptive optimization model whose solution is the set of cargo flows that satisfy, as best as possible given capacity limitations, the geographic demands for transport at minimum cost. There are two types of costs. The first cost is the transport cost of moving cargo across the arcs in the sea layer and/or road layer. Because the costs in the sea layer are significantly lower than the for the road layer, the model will primarily use the sea layer but revert to the road layer when necessary. The second cost is a per-unit penalty cost that is incurred for any cargo that is not delivered to its destination. In the event that significant disruption to the throughput capacity of a port or chokepoint makes it impossible to deliver cargo to a given destination, the model will suffer a high penalty. Overall, we set the costs so that the model will always deliver cargo if possible, even if it means incurring potentially high costs to do so.

This model is instrumented with binary parameters $\hat{x}_{ij}$ that make it easy for us to interdict individual arcs (i.e., make them cost prohibitive to use). By changing the value of $\hat{x}_{ij}$ for one or more arcs and then re-solving the model, we observe how cargo flows would reroute around the interdicted arcs. By iteratively changing these parameters and re-solving this model, we can systematically assess the potential impact of a variety of interdiction scenarios, which we detail in the next section.

Interdiction scenarios

We begin with an analysis of the system under normal operating conditions (i.e., no interdictions of ports or chokepoints), a situation we refer to as the base case. The total amount of cargo in the global network is 138,203,566 TEUs, and the corresponding “cost” to move this cargo is evaluated at \$93,584,947,771. In this base scenario, all cargo is delivered (i.e., there is no delivery shortfall) using the sea layer only (i.e., there is no need to use the road network to supplement delivery). The computation time for solving the base case on a personal laptop is approximately three seconds (ignoring preprocessing time to load data from various files and postprocessing time to generate figures, etc). The flow of the base case scenario is illustrated in Fig. 6 (top row), viewed from different perspectives. It reveals the main routes of cargo transportation, distinguishable by the thick arcs around the globe. The most highly frequented routes are (1) between North America and Europe across the Atlantic; (2) between Northern Europe and Asia across the Strait of Gibraltar, Suez Canal, Indian Ocean and the Strait of Malacca; (3) between North America and Asia across the Atlantic, Cape of Good Hope and the Indian Ocean; and (4) between North America and Asia across the Pacific Ocean.

We use this base case scenario as a reference for three particular disruptions scenarios of interest.

Interdiction of Suez Canal

The Suez Canal provides a vital means of transshipment between the Mediterranean Sea and the Indian Ocean, and its interdiction has the potential to create considerable disruption to global transport. With the Suez Canal interdicted, our model re-routes flows in a manner that minimizes the incremental cost. Figure 6 (2nd row) illustrates the resulting cargo flow, compared to the base case cargo flow in Fig. 6 (top row). The interdicted Suez Canal is highlighted by the red symbol in the middle figure. On the left, a slight increase of the flow between Asia and the Panama Canal can be detected, as well as an increased flow between North America and Europe. In the middle, where the Suez Canal is located, are the most significant changes. The flow between Europe and Asia across the Red Sea is completely interrupted and instead takes place over the Cape of Good Hope. The same applies for the flow between North America and Asia. On the right, we observe two effects. First, most of the cargo from Asia is directed to the Cape of Good Hope, instead of Bab-el-Mandeb (Mandeb Strait). Second, a greater portion of this flow traverses the Sunda Strait, instead of the Strait of Malacca.

Table 3 provides the results of the interdiction. The increase in the total transportation cost is \$6,355,097,051, which is about 6.8% of the base case cost. The reason for the increase is longer transportation routes from origin to destination. As seen in Fig. 6 (2nd row), there is one road transportation arc (in green) that is utilized between Ashdod, Israel and Jeddah, Saudi Arabia. But the amount of flow there is so small that none of the ports exhausts its capacity.

Interdiction of Panama Canal

The next scenario that we consider is an interdiction of the Panama Canal. Figure 6 (3rd row) shows the clear flow changes in this scenario. On the left, we recognize the decreased flow from Europe, but a significant increase from Cape of Good Hope to North America. Furthermore, the transition through the Strait of Magellan has become more important despite of the long way round for the most routes. In the middle, the huge increase of ow in the southern hemisphere between Asia and North America

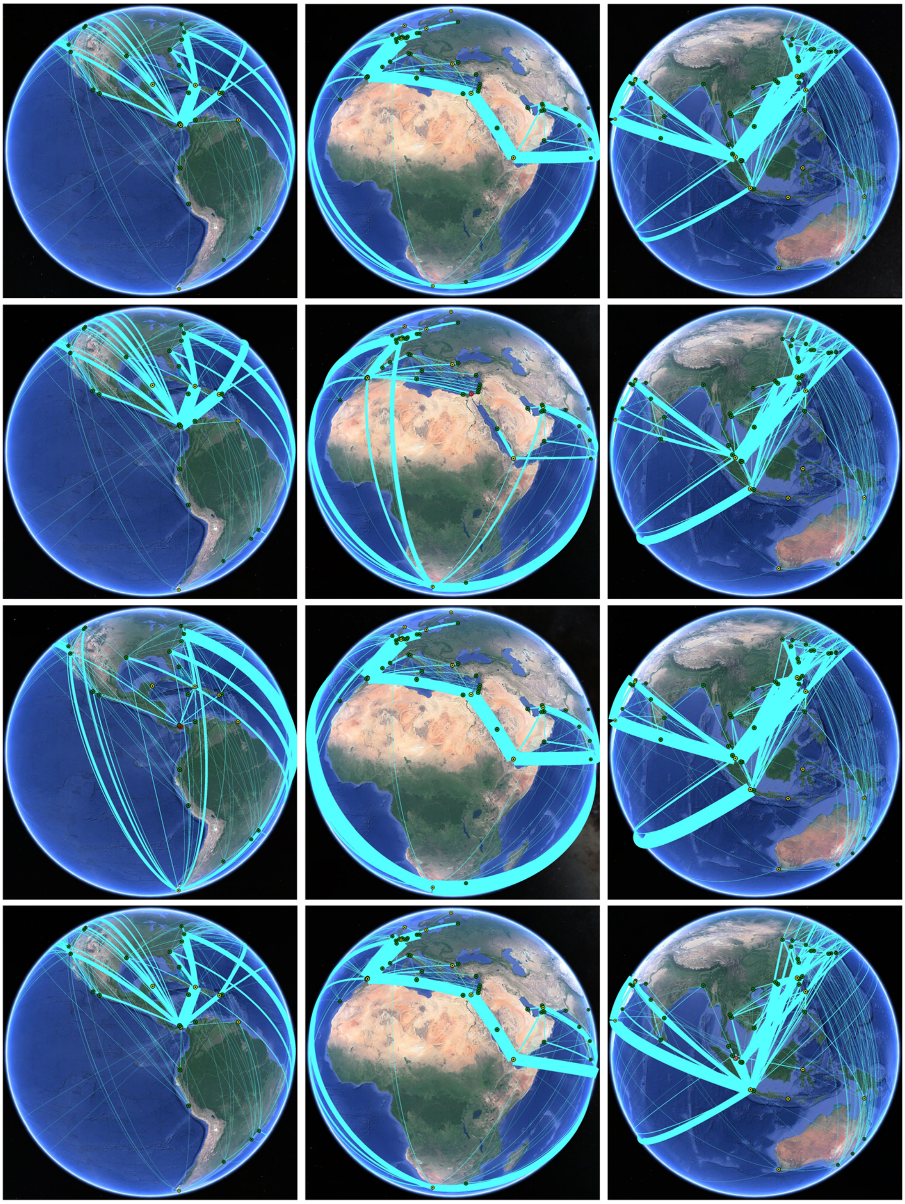

Fig. 6 Comparative results for Four Scenarios. Top Row: Base case scenario (no interdictions). Second Row: Suez Canal failure scenario. Third Row: Panama Canal failure scenario. Last Row: Straits of Malacca failure scenario

across the Indian Ocean and the Atlantic is clear to see. This is confirmed by the figures on the right, where the traffic through the Sunda Strait increased even more than in the previous scenario. A decrease of flow across the Pacific is also recognizable.

Table 3 shows the increased transportation cost in this scenario, which here is 10.3% higher than in the base case. On both ends of the Panama Canal (Pacific and the

Caribbean Sea) container ports are located in our model. These are the port of Balboa and the Manzanillo International Terminal. The increase of the road transportation portion of flow comes from increased cargo along the road connection between the two ports (until the port capacities are exhausted).

Interdiction of Strait of Malacca

The last single interdiction scenario we consider is a blockade of the Strait of Malacca. The effects of the interdiction are hardly recognizable in Fig. 6 (bottom row). In Asia (on the left), we observe a simple shift of traffic from the Strait of Malacca to the Sunda Strait. This result also appears in Table 3. The increase in the total transportation cost is approximately 2.2%, compared to the base case. There is no road transportation or ports with exhausted capacity result from the interdiction. The Sunda Strait seems to be a good substitute of the Strait of Malacca.

Identifying most critical nodes

We now consider a different question: which nodes, if interdicted, yield the biggest increase in system cost? Such nodes are often called the "most vital" or "most critical" nodes in the system (see Alderson et al. 2013, for brief history). To evaluate this, we exhaustively enumerate each possible scenario with exactly one interdicted port or maritime chokepoint. Table 4 lists the top ten nodes with greatest increase to the total transportation cost. The most expensive scenario is a failure of the port in Busan, which is the sixth biggest port in the world. If Busan is interdicted, all the cargo to and from this port is transported through the closest ports, which are far away and do not have sufficient capacity for this amount of redirected cargo. Therefore, three closest ports exhaust their capacity until all cargo demands are satisfied. This creates a lot of expensive road transportation and further increases the total cost of the scenario. Similar behavior is observed for scenarios associated with the interdiction of other ports in the table. Interdictions to maritime chokepoints result in less road transportation, in general, but they cause instead long detours and thus increase the total cost.

There are several single-node interdiction scenarios that result in a shortfall of cargo for some nodes. This happens mostly to interdicted ports on islands that don't have adjacent ports on the same island. Then there is no alternative route for transportation. Since our model sets a very high penalty cost on having a shortfall, it is not realistic to add this artificial cost to the total cost. But in reality, the penalty cost for undelivered

Table 3 Relative comparison of global flows between normal operations and three failure scenarios

	Base Case	Loss of Suez Canal	Loss of Panama Canal	Loss of Straits of Malacca
total transportation "cost"	$93,584,947,771	$99,940,044,822	$103,200,517,821	$95,682,578,400
total shortfall/excess	O TEU	O TEU	O TEU	O TEU
portion of road transportation	0%	0.1%	0.8%	0%
ports with exhausted capacity	0	0	2*	0

*Balboa, Panama; Manzanillo International Terminal, Panama cargo can still be very high. Table 5 provides an overview of the resulting shortfall in some scenarios.

We are now prepared to answer an important question: Are the most "critical" nodes, as indicated by our flow model, also the most "central" or the ones with the biggest throughput? Table 6 lists the twenty nodes whose loss results in the highest increase in total flow cost. For each node, we also list its rank as a "central" node, as defined by betweenness centrality, along with its rank in terms of annual throughput (for ports only). Although this table generally includes the most central nodes and the ports with the highest throughput, we observe that being a central node or a port with high throughput is not sufficient, on its own, to contribute to being a critical node. Specifically, we observe several ports, such as Savannah, Houston, Bandar Abbas, and Cartagena, that are neither among the top 20 most central nodes nor among the ports with the highest throughput but are critical from the flow perspective. This is often because there may not be nearby port alternatives in the event that these ports become disabled.

Multiple interdictions

As an extension to the previous analysis, we take a closer look at scenarios with multiple port interdictions. We expect that, depending on the combination of nodes that are affected, the total impact of multiple interdictions might be greater than just the sum of the single scenario impacts. If two closed ports are in the same area, they serve as substitutes for one another. This way, farther ports need to process cargo for multiple ports and the transportation cost might explode. In this subsection we only consider port failures, that is, we assume that maritime chokepoints are always available for use.

First, we evaluate a specific scenario that reminds of the West Coast port labor lockout in 2002. For the scenario, we close three major U.S. ports: Long Beach, Los Angeles and Oakland. These ports constitute a major portion in North America's West Coast logistics network. Since the ports have a big total cumulative throughput and they are located close to each other, we expect a lot of road transportation and therefore high cost.

Table 4 Nodes with the highest transportation cost increase compared to the base case

Rank	Closed node	Cost increase	Road portion	Exhausted ports
1	Busan	19.66%	5.79%	3
2	Strait of Gibraltar	15.45%	1.83%	3
3	Jawaharlal Nehru Port	11.50%	1.08%	3
4	Port of Shanghai	10.87%	4.14%	2
5	Panama Canal	10.27%	0.78%	2
6	Strait of Hormuz	9.16%	1.87%	0
7	New York	9.00%	2.18%	2
8	Bab-el-Mandeb	8.57%	0.11%	0
9	Shenzhen	8.16%	3.17%	2
10	Dubai	6.83%	1.61%	3

The resulting flow in Fig. 7 confirms our expectations. On the left, it shows many thick road transportation arcs across North America. All West Coast ports in Canada and Mexico are busy supporting the three ports. Even the ports at the east coast are involved in processing the cargo of the interdicted ports. Both other perspectives indicate an increase in sea transportation routes between North American's East Coast ports and both continents Europe and Asia.

The results in Table 7 emphasize the visual observation from the map. The road transportation flow has increased to 8.3%. Due to this fact, the total transportation cost in the scenario is 80.7% higher than in the base case. This increase in value is caused by just about 3% of the ports. Six container ports in Canada, Mexico and the U.S. exhaust their capacities while supporting the interdicted ports. Additional port failures in North America would most likely cause shortfalls because the cumulative capacity would be exhausted there.

Finding meaningful combinations of failing ports is a challenging task, because too many possible combinations exist to search exhaustively. Although the Attacker-Defender techniques in Alderson et al. (2014) could be used to identify worst-case interdictions without enumeration, we do not use them here. Instead, we restrict our analysis to exactly two concurrent failing ports and evaluate every possible combination to produce a ranking similar to that for single interdictions. Having 94 container ports in the model, this means considering a total of 4371 scenarios which takes about six days of total computation time.

Table 8 lists the twenty two-port combinations that cause the highest increase to transportation costs. The worst scenario by far is the scenario involving the failure of Long Beach and Los Angeles ports, which results in a 52.2% cost increase. The second and third positions, involving scenarios of failures in the Malay Peninsula and in China, are considerably less costly. In the further positions, the cost decrease smoothly towards the end of the table.

Although the highest value is caused by U.S. ports, the port of Busan is represented disproportionately in the first twenty positions. The reason is that this port caused the

Table 5 Single-node interdictions resulting in cargo shortfalls

Rank	Closed node	Total scenario shortfall (in TEU)
1	Tanjung Priok	4,460,000
2	Kaohsiung	2,865,533
3	Manila	2,148,180
4	Colombo	2,112,374
5	Marsaxlokk	1,352,232
6	Dublin	1,345,965
7	Tangier	1,237,929
8	Durban	1,124,715
9	Kingston	860,988
10	San Juan	764,339
11	Freeport	638,784
12	Las Palmas	555,731
13	Strait of Hormuz	4

Table 6 Comparing different indicators of node importance. For each of the top 20 most "critical" nodes, we list their rank in terms of being "central" or having the most port throughput (in TEUs). A '-' indicates that the node was not in the top 20. Chokepoints (listed in bold) do not have port throughput. In general, we observe that neither node centrality or node throughput is sufficient to predict criticality in terms of cargo flow

	RANK		
Node	Most "critical"	Most "central"	Most port throughput
Busan	1	18	4
Strait of Gibraltar	2	1	
Jawaharlal Nehru Port	3	–	26
Port of Shanghai	4	–	1
Panama Canal	5	6	
Strait of Hormuz	6	15	
New York	7	19	23
Bab-el-Mandeb	8	3	
Shenzhen	9	–	3
Dubai	10	–	8
Suez Canal	11	2	
Singapore	12	9	2
Savannah	13	–	39
Jeddah	14	–	27
Qingdao	15	–	7
Houston	16	–	66
Bandar Abbas	17	–	40
Tianjin	18	–	10
Cartagena	19	–	67
Øresund	20	–	

highest cost increase in the single interdiction scenarios. It is surprising that the worst two-port interdictions are not only ports that are located near to each other, but also include some combinations of ports from different continents. The highest road portion value of all scenarios is 8.75% and at most six ports exhaust their capacities in each scenario.

Increased use of Arctic Sea routes

The last analysis in this section concerns the Arctic sea routes. As mentioned earlier, the Northwest Passage and the Northeast Passage are currently usable only for a few months of a year because of the ice. Therefore, only a few ships per year choose these routes and therefore we have set an artificial capacity there at 18 ships per year. But due to climate change and melting arctic ice, the availability of these routes could increase. Then they would become more attractive for shipping companies, because in some cases they are shorter than the routes used today. To investigate this statement, we increase the capacity of the arctic routes and observe the resulting impact to the global transportation system. As an example, we decide for the current throughput of the port

Fig. 7 Comparison of the base and the West Coast ports failure scenario

of Los Angeles and implement it at the common entrance of both arctic routes—the Bering Strait.

The resulting cargo traffic is presented in Fig. 8. Not surprisingly, we observe that both Arctic arcs are utilized much more than in the base case. The figures in the left columns show, that the flow from Asia to the Panama Canal has decreased. In general, there exists less cargo between the Panama Canal and the U.S. East Coast. The East Coast is now supplied better by the Northwest Passage than before. The perspective on the right column substantiates the reduced ow between Asia and the Mediterranean Sea. A great portion of the flow from Asia is now directed to the Bering Strait and from there further to the arctic routes.

Table 9 shows the corresponding numbers of this last scenario. The total transportation cost is about 3.6% lower than in the base case scenario. This is a considerable savings of money and fuel for global transportation, if we assume the same transportation cost through the arctic routes as for all other routes. The result also shows that the scenario has exhausted the capacity of the Bering Strait. This means that the arctic routes most likely would carry even more cargo in the optimal solution, if we allow a higher capacity in the Bering Strait.

Conclusion and future work

This paper presents a multilayer network model that we use to study the structure and behavior of the GMTN. We analyze the network from a connectivity perspective and also construct a model of cargo flows that includes transportation costs and capacity constraints. We systematically assess the impact of closing one or more seaports and/or maritime chokepoints, and use this to identify the most "critical" nodes in the network.

Table 7 Result of the interdiction of the West Coast ports

Scenario Results Table	
total transportation cost	$169,079,946,490
total shortfall/excess	0 TEU
portion of road transportation	8.3%
ports with exhausted capacity	6*

*Houston, Lazaro Cardenas, Manzanillo, Metro Vancouver, Savannah, Seattle

Table 8 Highest cost increase for double interdictions

rank	closed node	cost increase	road portion	exhausted ports
1	Long Beach, Los Angeles	52.20%	5.98%	6
2	Port Klang, Singapore	36.38%	5.71%	6
3	Guangzhou, Shenzhen	33.25%	4.17%	2
4	Ningbo, Port of Shanghai	32.95%	5.35%	4
5	New York, Savannah	30.44%	3.46%	4
6	Busan, Port of Shanghai	29.90%	8.75%	5
7	Singapore, Tanjung Pelepas	29.31%	5.02%	5
8	Busan, New York	28.67%	6.71%	5
9	Busan, Shenzhen	27.82%	7.61%	5
10	Busan, Dalian	27.69%	6.02%	3
11	Busan, Kwangyang	27.53%	6.34%	3
12	Busan, Tianjin	26.73%	7.13%	4
13	Busan, Dubai	26.50%	6.45%	6
14	Busan, Incheon	25.71%	5.94%	3
15	Busan, Singapore	25.21%	8.61%	5
16	Busan, Savannah	25.11%	5.96%	4
17	Busan, Qingdao	24.89%	6.42%	4
18	Busan, Houston	24.70%	5.68%	3
19	Hampton Roads, New York	23.78%	2.89%	3
20	Busan, Cartagena, New York	23.51%	5.28%	4

We also show how this framework can be used to consider other "what-if" types of questions, such as increased transportation capacity through the Arctic Circle. We show that this type of analysis provides realistic, insightful, and computationally tractable results regarding the security and resilience of the GMTN. Yet, there is considerable room for improvements and additional research.

First, this analysis would benefit from data that is more detailed and more realistic. Although we were able to construct a relatively complete picture of global flows using data from public sources, there exist private databases (commensurate with the data used by global shipping companies to manage these operations) that would enable a more accurate view of current operations and potential contingencies in the face of a major disruptive event.

Second, there are considerably more operational constraints than are represented here. For example, sea transport is often closely coordinated with landside connections such that it might not be logistically feasible or cost effective for a container ship to divert to an alternative port. Although we differentiate cargo commodity by destination, we do not consider different types of cargo. In practice, for example, refrigerated cargo has additional constraints both at sea and ashore. And there may be different priorities of cargo that need to be considered when modeling port operations. Moreover, the operations within a port have additional dependencies that include, among other things, the availability of individual cranes and terminals. Thus, disruptions within a port are not simply binary as represented here, and additional work is required to understand

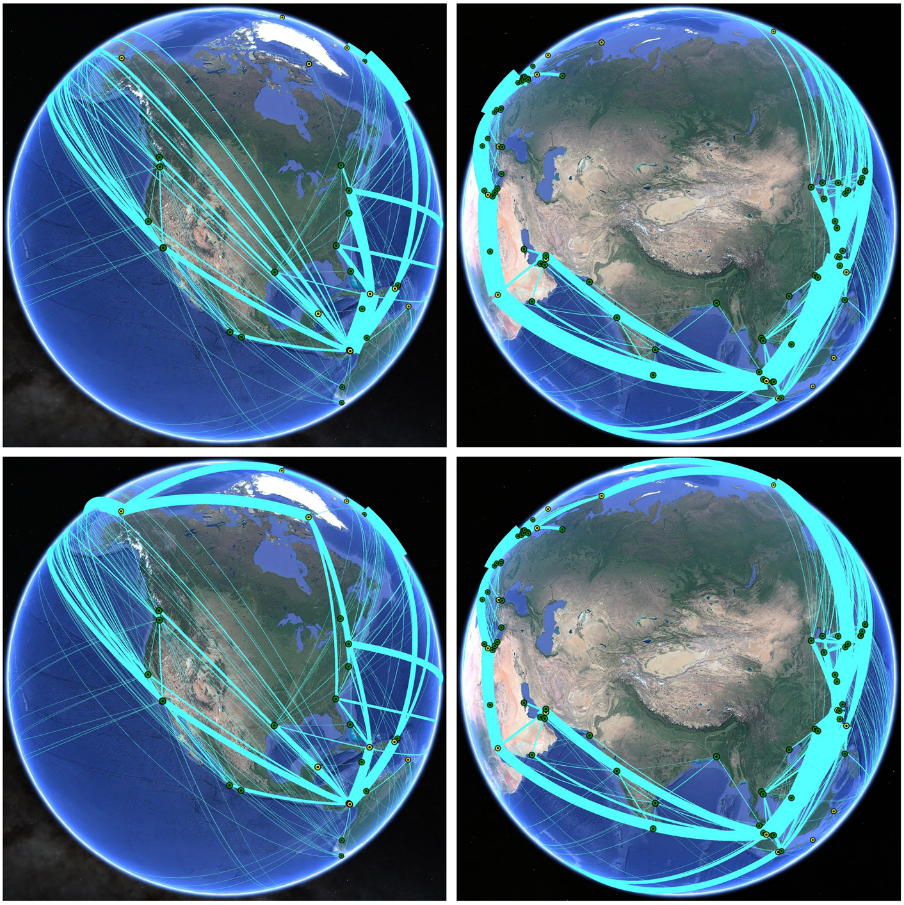

Fig. 8 Comparison of the base case (top row) and the increased availability of Arctic routes (botton row)

how the loss of different sets of components can adversely affect port operations; see De la Cruz (2011), Mintzer (2014), or Wenke (2015) for examples.

Third, ongoing pressure for economies of scale is driving the design of bigger and bigger cargo ships, with the newest Ultra Large Container Vessel ships now able to be serviced at only a few megaports (further separating them from the others). In practice, it might not be possible for these ships to go elsewhere (thus resulting in more systemwide fragility). Understanding the tensions between this ongoing drive for

Table 9 Results of the increased capacity in the arctic sea routes

Scenario Results Table	
total transportation cost	$90,178,602,508
total shortfall/excess	0 TEU
portion of road transportation	0%
ports with exhausted capacity	–

"faster, better, cheaper" transport and the need for a system that is resilient in the face of surprise is a topic of open investigation.

Finally, understanding the potential impact of Arctic sea opening, sea level rise, and other climatic changes serve as potentially fruitful and important avenues for future research.

Acknowledgments This manuscript is adapted from the thesis by one of the authors (Funk 2017), and portions of this work have appeared there. The authors would like to thank Stephen Flynn for ongoing conversations about the security and resilience of the maritime transport system. This research was funded in part by the Office of Naval Research and the Defense Threat Reduction Agency.

Appendix. Additional Data Tables

Table 10 Exports and imports of the countries of the model. Source: Central intelligence Agency (2017)

Country	Exports	Imports
Argentina	$58.4 billion	$57.23 billion
Australia	$184.3 billion	$203.1 billion
Bahamas	$880 million	$2.495 billion
Bangladesh	$33.32 billion	$39.17 billion
Belgium	$250.8 billion	$251.7 billion
Brazil	$189.7 billion	$143.9 billion
Canada	$402.4 billion	$419 billion
China	$2.011 trillion	$1.437 trillion
Colombia	$33.64 billion	$47.15 billion
Ecuador	$16.77 billion	$17.74 billion
Egypt	$14.73 billion	$50.07 billion
France	$505.4 billion	$5252.4 billion
Germany	$1.283 trillion	$987.6 billion
India	$271.6 billion	$402.4 billion
Indonesia	$136.7 billion	$121.5 billion
Iran	$87.52 billion	$62.12 billion
Ireland	$160.1 billion	$88.01 billion
Israel	$51.61 billion	$57.9 billion
Italy	$436.3 billion	$372.2 billion
Jamaica	$1.278 billion	$ 3.772 billion
Japan	$641.4 billion	$629.8 billion
Korea, South	$509 billion	$405.1 billion
Lebanon	$3.108 billion	$17.98 billion
Malaysia	$167.3 billion	$139.5 billion
Malta	$2.915 billion	$4.479 billion
Mexico	$359.3 billion	$372.8 billion

Table 10 (continued)

Country	Exports	Imports
Morocco	$18.72 billion	$33.15 billion
Netherlands	$460.1 billion	$376.3 billion
Oman	$30.39 billion	$25.78 billion
Pakistan	$20.96 billion	$38.25 billion
Panama	$15.19 billion	$22.08 billion
Peru	$38.09 billion	$38.35 billion
Philippines	$38.2 billion	$60.95 billion
Puerto Rico	$70.41 billion	$47.61 billion
Russia	$259.3 billion	$165.1 billion
Saudi Arabia	$205.3 billion	$157.7 billion
Singapore	$353.3 billion	$271.3 billion
South Africa	$83.16 billion	$85.03 billion
Spain	$266.3 billion	$287.9 billion
Sri Lanka	$10.12 billion	$18.64 billion
Taiwan	$314.8 billion	$248.7 billion
Thailand	$190 billion	$171.3 billion
Turkey	$150.1 billion	$197.8 billion
United Arab Emirates	$316 billion	$246.9 billion
United Kingdom	$412.1 billion	$581.6 billion
United States	$1.471 trillion	$2.205 trillion
Vietnam	$169.2 billion	$161 billion

Table 11 Main export and import partners of the countries. Source: Central Intelligence Agency (2017)

Country	Export Partners	Import Partners
Argentina	Brazil 17%, China 8.6%, US 5.9%	Brazil 22.4%, US 16.3%, China 15.5%, Germany 5.1%
Australia	China 32.2%, Japan 15.9%, South Korea 7.1%, US 5.4%, India 4.2%	China 23%, US 11.2%, Japan 7.4%, South Korea 5.5%, Thailand 5.1%, Germany 4.6%
Bahamas	US 15.9%	US 22.3%, China 14.8%, Japan 9.5%, South Korea 7.3%, Columbia 6.8%, Brazil 5.6%, Singapore 5.5%
Bangladesh	US 13.9%, Germany 12.9%, France 5%, Spain 4.7%	China 22.4%, India 14.1%, Singapore 5.2%
Belgium	Germany 16.9%, France 15.5%, Netherlands 11.4%, UK 8.8%, US 6%, Italy 5%	Netherlands 16.7%, Germany 12.7%, France 9.6, US 8.7%, UK 5.1%, Ireland 4.7%, China 4.3%
Brazil	China 18.6%, US 12.7%, Argentina 6.7%, Netherlands 5.3%	China 17.9%, US 15.6, Germany 6.1%, Argentina 6%
Canada	US 76.7%	US 53.1%, China 12.2%, Mexico 5.8%
China	US 18%, Japan 6%, South Korea 4.5%	South Korea 10.9%, US 9%, Japan 8.9%, Germany 5.5%, Australia 4.1%
Colombia	US 27.5%, Panama 7.2%, China 5.2%, Spain 4.4%, Ecuador 4%	US 28.8%, China 18.6%, Mexico 7.1%, Germany 4.2%
Ecuador	US 39.5%, Peru 5.1%, Vietnam 4.3%, Colombia 4.3%	US 27.1%, China 15.3%, Colombia 8.3% Panama 4.9%
Egypt	Saudi Arabia 9.1%, Italy 7.5%, Turkey 5.8%, UAE 5.1%, US 5.1%, UK 4.4%, India 4.1%	China 13%, Germany 7.7%, US 5.9%, Turkey 4.5%, Russia 4.4%, Italy 4.4%, Saudi Arabia 4.1%
France	Germany 15.9%, Spain 7.3%, US 7.2%, Italy 7.1%, UK 7.1%, Belgium 6.8%	Germany 19.5%, Belgium 10.7%, Italy 7.7%, Netherlands 7.5%, Spain 6.8%, US 5.5%, China 5.4%, UK 4.3%
Germany	US 9.6%, France 8.6%, UK 7.5%, Netherlands 6.6%, China 6%, Italy 4.9%	Netherlands 13.7%, France 7.6%, China 7.3%, Belgium 6%, Italy 5.2%, US 4.7%, UK 4.2%
India	US 15.2%, UAE 11.4%	China 15.5%, Saudi Arabia 5.4%, US 5.2%
Indonesia	Japan 12%, US 10.8%, China 10%, Singapore 8.4%, India 7.8%, South Korea 5.1%, Malaysia 5.1%	China 20.6%, Singapore 12.6%, Japan 9.3%, Malaysia 6%, South Korea 5.9%, Thailand 5.7%, US 5.3%
Iran	China 22.2%, India 9.9%, Turkey 8.4%, Japan 4.5%	UAE 39.6%, China 22.4%, South Korea 4.7%, Turkey 4.6%

Table 11 (continued)

Country	Export Partners	Import Partners
Ireland	US 23.7%, UK 13.8%, Belgium 13.2%, Germany 6.6%, Netherlands 4.4%, France 4.4%	UK 32.5%, US 14%, France 10.2%, Germany 9.3%, Netherlands 4.9%, China 4.1%
Israel	US 27.5%, UK 6.1%, China 4.9%	US 13%, China 9.3%, Germany 6.1%, Belgium 5.3%, Italy 4%
Italy	Germany 12.3%, France 10.3%, US 8.7%, UK 5.4%, Spain 4.8%	Germany 15.4%, France 8.7%, China 7.7%, Netherlands 5.6%, Spain 5%, Belgium 4.7%
Jamaica	US 24.4%, Canada 16.5%, Russia 9.3%, Netherlands 8.9%, UK 6.5%	US 32.6%, China 12%
Japan	US 20.2%, China 17.5%, South Korea 7.1%, Thailand 4.5%	China 24.8%, US 10.5%, Australia 5.4%, South Korea 4.1%
Korea, South	China 26%, US 13.3%, Vietnam 5.3%, Japan 4.9%	China 20.7%, Japan 10.5%, US 10.1%, Germany 4.8%, Saudi Arabia 4.5%
Lebanon	Saudi Arabia 12.1%, UEA 10.6%, South Africa 6.6%	China 11.5%, Italy 7.1%, Russia 4.6%
Malysia	Singapore 13.9%, China 13%, Japan 9.5%, US 9.4%, Thailand 5.7%, India 4.1%	China 18.8%, Singapore 12%, US 8.1%, Japan 7.8%, Thailand 6.1%, South Korea 4.5%, Indonesia 4.5%
Malta	Germany 13.3%, France 10.2%, Singapore 7.3%, UK 6.4, US 5.8%, Italy 5.6%, Japan 4.7%	Italy 23%, Netherland 8.4%, UK 7.5%, Germany 6.8%, Canada 6.1%, China 4.1%, France 4%
Mexico	US 81.1%	US 47.3%, China 17.7%, Japan 4.4%
Morocco	Spain 22.1%, France 19.7%, India 4.9%, Italy 4.3%	Spain 13.9%, France 12.4%, China 8.5%, US 6.5%, Germany 5.8%, Italy 5.5%, Russia 4.4%, Turkey 4.3%
Netherlands	Germany 24.5%, Belgium 11.1%, UK 9.3%, France 8.4%, Italy 4.2%	Germany 14.7%, China 14.5%, Belgium 8.2%, US 8.1%, UK 5.1%
Oman	China 35.4%, UAE 15.3%, South Korea 6.8%, Saudi Arabia 5.8%, Pakistan 4.2%	UAE 29.7%, Japan 10.2%, US 7.5%, China 6.7%, India 6.3%
Pakistan	US 13.1%, UAE 9.1%, China 8.8%, UK 5.4%, UK 5.4%, Germany 4.9%	China 28.1%, Saudi Arabia 10.9%, UAE 10.8%
Panama	US 25.9%, Germany 13.2%, China 5.9%, Netherlands 4.1%	US 25.9%, China 9.6%, Mexico 5.1%
Peru	China 22.1%, US 15.2%, Canada 7%	China 22.7, US 20.7%, Brazil 5.1%, Mexico 4.5%
Philippines	Japan 21.1%, US 15%, China 10.9%, Singapore 6.2%, Germany 4.5%, South Korea 4.3%	China 16.2%, US 10.8%, Japan 9.6%, Singapore 7%, South Korea 6.5%, Thailand 6.4%, Malaysia 4.8%, Indonesia 4.4%

Table 11 (continued)

Country	Export Partners	Import Partners
Puerto Rico	Canada 18.6%, Mexico 15.7%, China 7.7%, Japan 4.2%	China 21.5%, Canada 13.2%, Mexico 13.2%, Japan 5.9%, Germany 5.5%
Russia	Netherlands 11.9%, China 8.3, Germany 7.4%, Italy 6.5%, Turkey 5.6%, Japan 4.2%	China 19.2%, Germany 11.2%, US 6.4, Italy 4.6
Saudi Arabia	China 13.2%, Japan 10.9%, US 9.6%, India 9.6%, South Korea 8.5%	China 13.9%, US 12.7%, Germany 7.1%, South Korea 6.1%, India 4.5%, Japan 4.4%, UK 4.3%
Singapore	China 13.7%, Malaysia 10.8%, Indonesia 8.2%, US 6.9%, Japan 4.4%, South Korea 4.1%	China 14.2%, US 11.2%, Malaysia 11.2%, Japan 6.3%, South Korea 6.1%, Indonesia 4.8%
South Africa	China 11.3%, US 7.3%, Germany 6%, Japan 4.7%, UK 4.3%, India 4.2%	China 17.6%, Germany 11.2%, US 6.7%, India 4.7%, Saudi Arabia 4.1%
Spain	France 15.7%, Germany 11%, Italy 7.4%, UK 7.4%, US 4.5%	Germany 14.4%, France 11.7%, China 7.1%, Italy 6.5%, Netherlands 5%, UK 4.9%
Sri Lanka	US 26%, UK 9%, India 7.2%, Germany 4.3%	India 24.6%, China 20.6%, UAE 7.2%, Singapore 5.9%, Japan 5.7%
Taiwan	China 27.1%, US 10.3%, Japan 6.4%, Singapore 4.4%	Japan 17.6, China 16.1%, US 9.5%
Thailand	US 11.2%, China 11.1%, Japan 9.4%, Malaysia 4.8%, Australia 4.6%, Vietnam 4.2%, Singapore 4.1%	China 20.3%, Japan 15.4%, US 6.9%, Malaysia 5.9%, UAE 4%
Turkey	Germany 9.3%, UK 7.3%, Italy 4.8%, US 4.5%, France 4.1%	China 12%, Germany 10.3%, Russia 9.9%, US 5.4%, Italy 5.1%
UAE	Iran 14.5%, Japan 9.8%, India 9.2%, China 4.7%, Oman 4.3%	China 15.7%, India 12.8%, US 9.7%, Germany 6.8%, UK 4.4%
UK	US 14.6%, Germany 10.1%, China 6%, France 5.9%, Netherlands 5.8%, Ireland 5.5%	Germany 14.8%, China 9.8%, US 9.2%, Netherlands 7.5%, France 5.8%, Belgium 5%
US	Canada 18.6%, Mexico 15.7%, China 7.7%, Japan 4.2%	China 21.5%, Canada 13.2%, Mexico 13.2%, Japan 5.9%, Germany 5.5%
Vietnam	US 21.2%, China 13.3%, Japan 8.4%, South Korea 5.5%, Germany 4.1%	China 34.1%, South Korea 14.3%, Singapore 6.5%, Japan 6.4%, Thailand 4.5%

References

Ahuja RK, Magnanti TL, Orlin JB (1993) Network flows: theory, algorithms, and applications. Prentice Hall

Alderson D, Doyle J (2010) Contrasting views of complexity and their implications for network-centric infrastructures. IEEE Trans Sys Man Cybernetics A: Systems And Humans 40(4):839–852

Alderson DL (2008) Catching the "network science" bug: insight and opportunity for the operations researcher. Oper Res 56(5):1047–1065

Alderson DL, Brown GG, Carlyle WM (2014) Assessing and improving operational resilience of critical infrastructures and other systems. In: Newman A, Leung J (eds) Tutorials in Operations Research: Bridging Data and Decisions. INFORMS, 180–215

Alderson DL, Brown GG, Carlyle WM (2015) Operational models of infrastructure resilience. Risk Anal 35(4):562–586

Alderson DL, Brown GG, Carlyle WM, Cox LA (2013) Sometimes there is no "most vital" arc: assessing and improving the operational resilience of systems. Mil Oper Res 18(1):21–37

Basu P, Sundaram R, Dippel M (2015) Multiplex networks: a generative model and algorithmic complexity. Proceedings of the 2015 IEEE/ACM International Conference on Advances in Social Networks Analysis and Mining 2015. ACM, 456–463

Bencomo LA (2009) Modeling the effects of a transportation security incident on the commercial transportation system. Master's thesis, Naval Postgraduate School, Monterey, California

Brin S, Page L (2012) Reprint of: the anatomy of a large-scale hypertextual web search engine. Comput Netw 56(18):3825–3833

Brown GG, Carlyle WM, Salmerón JS, Wood RK (2006) Defending critical infrastructure. Interfaces 36:530–544

Brown GG, Washburn AR (2017) Method and system for determining shortest oceanic routes. United States patent 9,541,401. Issued 10 January

Bruns S, Petretto K, Petrovic D (2013) Maritime Sicherheit [maritime security] . Springer-Verlag

Cardillo A, Zanin M, Gómez-Gardenes J, Romance M, del Amo AJ, Boccaletti S (2013) Modeling the multi-layer nature of the European air transport network: resilience and passengers re-scheduling under random failures. The European Physical Journal Special Topics 215(1):23–33

Central Intelligence Agency (2017) The world factbook. URL https://www.cia.gov/library/publications/the-world-factbook/. Accessed February 2017

Chen L, Miller-Hooks E (2012) Resilience: an indicator of recovery capability in intermodal freight transport. Transp Sci 46(1):109–123

Cohen SS (2002) Economic impact of a west coast dock shutdown. University of California at Berkeley 1

Cruz A (2016) Bankruptcy woes: Hanjin makes waves across the world. Global trade http://www.globaltrademag.com/global-logistics/bankruptcy-woes-hanjin-makes-waves-across-world. Accessed 4 Dec 2017

De Domenico M, Lancichinetti A, Arenas A, Rosvall M (2015) Identifying modular flows on multilayer networks reveals highly overlapping organization in interconnected systems. Physical Review X 5(1): 011027

De la Cruz CF (2011) Defending the maritime transport of cargo for the Hawaiian islands. Master's thesis, Naval Postgraduate School, Monterey, CA

Drake JM, Lodge DM (2007) Hull fouling is a risk factor for intercontinental species exchange in aquatic ecosystems. Aquat Invasions (2)

Ducruet C, Notteboom T (2012) The worldwide maritime network of container shipping: spatial structure and regional dynamics. Global networks 12(3):395–423

Faturechi R, Miller-Hooks E (2014) Measuring the performance of transportation infrastructure systems in disasters: a comprehensive review. J Infrastruct Syst 21(1):04014025

Flynn SE, Holmes J, Burke S (2017) A new international framework for bolstering global supply system security and resilience. Tech. rep., Global Resilience Institute, Northeastern University, Boston, MA

Freeman LC (1977) A set of measures of centrality based on betweenness. Sociometry 35-41

Funk D (2017) Analysis of the global maritime transportation system and its resilience. Master's thesis, Naval Postgraduate School, Monterey, CA

Garcia Olalla OR (2012) Assessing the resilience of global sea routes. Master's thesis, Naval Postgraduate School, Monterey, CA

Google (2017) Google Maps. URL http://www.maps.google.com/. Accessed December 04, 2017

Guimerá R, Amaral LAN (2004) Modeling the world-wide airport network. The European Physical Journal B 38(2):381–385

Guimerá R, Mossa S, Turtschi A, Amaral LAN (2005) The worldwide air transportation network: anomalous centrality, community structure, and cities' global roles. Proc Natl Acad Sci 102(22):7794–7799

Hirsch JE (2005) An index to quantify an individual's scientific research output. Proc Natl Acad Sci U S A 102(46):16569

Huber T (2014) "Global Ports" in der maritimen Transportwirtschaft. Akteursbasierende Bewertung des weltweiten Netzwerks von Hafenstandorten ["global ports" in the maritime transport sector, a player based assessment of the global network of port locations]. Ph.D. thesis, Fakultt fr Philosphie, Kunst-, Geschichts- und Gesellschaftswissenschaften der Universitt Regensburg, Regensburg, Germany

Jiang J, Lee LH, Chew EP, Gan CC (2015) Port connectivity study: an analysis framework from a global container liner shipping network perspective. Transportation Research Part E: Logistics and Transportation Review 73:47–64

Kaluza P, Klzsch A, Gastner MT, Blasius B (2010) The complex network of global cargo ship movements. J R Soc Interface 7(48):1093–1103

Katz L (1953) A new status index derived from sociometric analysis. Psychometrika 18(1):39–43

Khouri A (2015) West coast ports facing shutdown in labor dispute. Los Angeles Times https://www.latimes.com/business/la-fi-port-shutdown-20150207-story.html. Accessed 29 May 2017

Komiss W, Huntzinger L (2011) The economic implications of disruptions to maritime oil chokepoints. Center for Naval Analysis

Madhusudan C, Ganapathy GP (2011) Disaster resilience of transportation infrastructure and ports: an overview. International Journal of Geomatics and Geosciences 2(2):443

Martagan TG, Eksioglu B, Eksioglu SD, Greenwood AG (2009) A simulation model of port operations during crisis conditions. Proceedings of the 2009 Winter Simulation Conference (WSC), 2832–2843

Microsoft Corporation (2017) Bing Maps. http://www.bing.com/maps. Accessed December 04, 2017

Miller-Hooks E, Zhang X, Faturechi R (2012) Measuring and maximizing resilience of freight transportation networks. Comput Oper Res 39(7):1633–1643

Mintzer DS (2014) Optimizing the resilience of containerized cargo transportation infrastructure in the port of Los Angeles. Master's thesis, Naval Postgraduate School, Monterey, CA

Mitchell R (2015) Web scraping with Python: collecting data from the modern web. O'Reilly Media, Inc.

Nagurney A (2006) Supply chain network economics: dynamics of prices, flows and profits. Edward Elgar Publishing

Newman M (2010) Networks: an introduction. Oxford University Press, Oxford

Noer JH, Gregory D (1996) Chokepoints: maritime economic concerns in Southeast Asia. Tech. rep. DTIC Document

Onuska JJ (2012) Defending the Pittsburgh waterways against catastrophic disruption. Master's thesis, Naval Postgraduate School, Monterey, CA

Pidgeon ED (2008) Modeling the effects of a transportation security incident upon the marine transportation system. Master's thesis, Naval Postgraduate School, Monterey, CA

Rodrigue J-P, Comtois C, Slack B (2017) The geography of transport systems (4th Ed.). Taylor & Francis

Ruiz GM, Rawlings TK, Dobbs FC, Drake LA, Mullady T, Huq A, Colwell RR (2000) Global spread of microorganisms by ships. Nature 408(6808):49–50

Sabidussi G (1966) The centrality index of a graph. Psychometrika 31(4):581–603

SeaRates LP (2017) SeaRates.com: Digital Broker & Freight Forwarder. URL http://www.searates.com. Last accessed December 04, 2017

Shaw ME (1954) Some effects of unequal distribution of information upon group performance in various communication nets. The journal of abnormal and social psychology 49 (4p1) 547

Stephenson K, Zelen M (1989) Rethinking centrality: methods and examples. Soc Networks 11(1):1–37

The Tioga Group, Inc (2010) Container port capacity study. Report submitted to the US Army Corps of Engineers. Institute for Water Resources, Alexandria

Wang C, Wang J (2011) Spatial pattern of the global shipping network and its hub-and-spoke system. Res Transp Econ 32(1):54–63

Wang Y, Cullinane K (2016) Determinants of port centrality in maritime container transportation. Transportation Research Part E: Logistics and Transportation Review 95:326–340

Wenke W (2015) Assessing the operational resilience of the port of Anchorage: recommendations for investment and implications for policy. Master's thesis, Naval Postgraduate School, Monterey, CA

World Trade Organization (2007) World trade report. World Trade Organization
Zeihan P (2014) The accidental superpower: the next generation of American preeminence and the coming global disorder. Twelve, New York

Publisher's note Springer Nature remains neutral with regard to jurisdictional claims in published maps and institutional affiliations.